



Publication Year	2023
Acceptance in OA @INAF	2024-02-19T13:49:17Z
Title	Status of a C-band Phased Array Feed with RFSoc digital beamformer
Authors	PISANU, Tonino; MAXIA, PAOLO; CABRAS, Alessandro; SCHIRRU, Luca; ORTU, Pierluigi; et al.
DOI	10.23919/URSIGASS57860.2023.10265543
Handle	http://hdl.handle.net/20.500.12386/34774
Journal	...URSI GENERAL ASSEMBLY AND SCIENTIFIC SYMPOSIUM



Status of a C-band Phased Array Feed with RFSoc digital beamformer

T. Pisanu(1), P. Maxia(1), A. Cabras(1), L. Schirru(1), P. Ortu(1), A. Melis(1), A. Navarrini(1), M. Belluso(3), S. Billotta(3), G. Comoretto(2), R. Concu (1), P. Di Ninni(2), A. Ladu(1), P. Marongiu(1), R. Nesti(2).

(1) INAF (National Institute for Astrophysics)-Astronomical Observatory of Cagliari, Selargius, Italy

(2) INAF (National Institute for Astrophysics)-Arcetri Astrophysical Observatory, Florence, Italy

(3) INAF (National Institute for Astrophysics)-Catania Astronomical Observatory, Catania, Italy

Abstract

In this paper, we describe the design and development status of a room-temperature C-band Phased Array Feed (PAF) demonstrator, based on Radio Frequency System-on-Chip (RFSoc) for radio astronomy application, to be installed on the Sardinia Radio Telescope. The instrument is optimized to work across the 4.75- 6.00 GHz radio frequency (RF) band. The project of the front-end includes a compact RF module based on an 8×8 array of linear dual-polarization antenna elements integrated with Monolithic Microwave Integrated Circuit (MMIC) Low Noise Amplifiers (LNAs). In the preliminary version of the front-end project, which considers only one linear polarization, a subset of 32 elements are connected to the LNAs, while the rest of them are terminated to 50 Ohm matched loads. A dedicated signal acquisition chain of microwave components, based on two stages of filtering and signal conditioning, permits the injection of the 32 RF signals to the two commercial back-ends based on RFSoc digital boards. Each board is equipped with 16 inputs, with 1.25 GHz instantaneous bandwidth, and performs the frequency channelization, the partial and final beamforming of at least four independent beams (the number of beams may vary depending on the observation requirements). A general description of the front-end design, the back-end hardware, firmware and software development and an optimizer for the whole system performances evaluation, is presented.

1 Introduction

High-sensitivity large-scale surveys are an essential tool for new discoveries in radio astronomy. Thanks to a phased array feed (PAF) placed at the focal plane of a reflector antenna, it is possible to increase the Field-of-View (FoV) and the mapping efficiency by fully sampling the sky [1],[2],[3]. A PAF consists of closely packed antenna elements with about half wavelength element separation that, by spatially sampling the focal plane, can synthesize multiple independent beams and be set to Nyquist-sample the sky [4]. Multiple beams can be formed by electronically adding the signals from different groups of radiating elements of the array, using a dedicated beam-forming software installed on the digital back-end. An antenna element can contribute to forming multiple beams. The properties of the beams can be optimized over a wide range of frequencies by electronically controlling each element phase and amplitude (complex weights) leading to

high aperture efficiency and low spillover, in order to optimize the electromagnetic features of the reflector antenna where the PAF is installed. Several PAFs are available in the literature [5-6].

Recently, the Italian National Institute for Astrophysics (INAF) has contributed to developing the PAFs state-of-the-art, by presenting the instrument named PHAROS2, for which a detailed description is reported in [4], [7], [8], [9], [10]. This is based on the PHAROS (PHased Arrays for Reflector Observing Systems) cryogenically cooled C-band PAF demonstrator with analogue beam-former and on its upgrade (aptly named PHAROS2), utilizing a Warm Section (WS) multi-element downconverter [4], and a digital dedicated back-end based on the iTPM Italian Tile Processing Module.

In this paper, we describe the design and development status of a new PAF demonstrator, which operates in a portion of the C-band (4.75-6.00 GHz) at room temperature, equipped with a digital beam-former, capable of delivering an instantaneous bandwidth of 1.25 GHz [10]. This PAF will be installed on the Sardinia Radio Telescope (SRT), a fully steerable multi-reflector antenna designed to operate with high efficiency across the 0.3–116 GHz frequency range, which represents one of the Italian radio telescopes of ownership of the INAF and in particular of the Astronomical Observatory of Cagliari (OAC) [11]. The design of the new PAF takes advantage of the performance of the Xilinx Zynq UltraScale+ RFSoc technology as a back-end, which currently allows signal digitization and processing with a maximum input frequency of 6 GHz. Unlike the PHAROS2 front-end, which adopts a Warm Section, the new PAF architecture allows direct sampling of the RF signals, thus eliminating the down-conversion block, with great benefits in terms of engineering complexity, mechanical compactness, and costs [10].

The system's front-end and back-end are described in Section 2 and Section 3, respectively. In addition, a study regarding adaptive beam-forming using deep-learning techniques is presented in Section 4. Finally, a state-of-the-art analysis for an optimizer that evaluates the whole performance of the system is described in Section 5.

2 The design of the front-end

The front-end module consists of an 8×8 array of linear dual-polarization elements, integrated with MMIC LNAs.

In the next future, the design will consider the aspects related to the cryogenic operation, in view of upgrading this

system to a cryogenic broadband 3.0-7.7 GHz low-noise PAF with more than 30 dual-polarization beams and with more than 1 GHz bandwidth, as required to perform high-sensitivity large scale radio astronomy surveys with large single-dish radio telescopes like SRT. For this reason, the bandwidth considered in the array design is larger than the nominal frequency band of the PAF system (4.75- 6.00 GHz).

The front-end is equipped with an array of 64 dual-polarization antenna elements. Each element consists of two Vivaldi antennas for a total of 128 antennas. In this preliminary step, only 32 of the 128 array antennas (8x8x2 polarizations) are active (see Figure 1) and consequently connected to the receiver chain that leads to the back-end, while all the remaining ones are terminated to 50 Ω matched loads.

The single antenna element of the array is an aluminum broadband Vivaldi antenna [13-14], designed to operate in C-band (3.0-7.7 GHz) [10]: the spacing between two consecutive Vivaldi antennas is $\lambda/2$ at the shortest operative wavelength (19.48 mm).

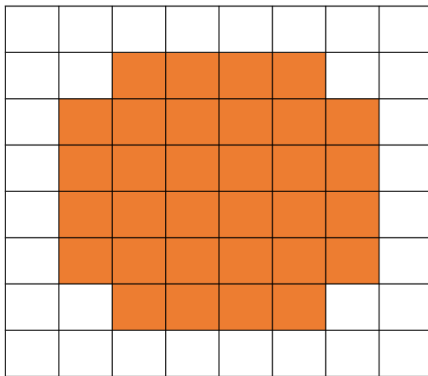


Figure 1: Simplified schematic of 8x8 elements array.

The flare length and the taper rate will be determined in order to obtain a 140° -5dB-beamwidth in the range 4.75-6 GHz with the aim to achieve an edge over-illumination of the 64 meters diameter reflector of SRT [11].

A first 3D electromagnetic model of the Vivaldi array was created with the commercial software CST microwave studio (see Figure 2).

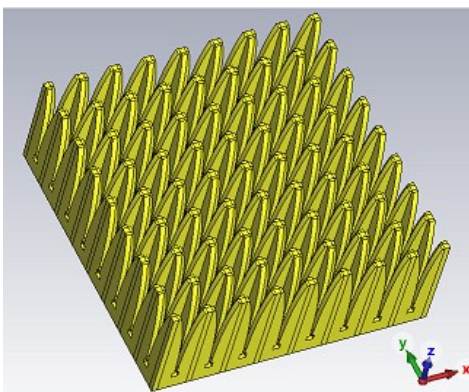


Figure 2: 3D view of the CST model of the C-band PAF.

Each of the active elements is integrated with MMIC LNAs, as shown in the schematic of Figure 3. The LNA is the NEC NE3515502 model, with a gain of about 13 dB and a noise figure of about 0.3 dB. The performances of this LNA model are essential for determining a low noise figure of the whole system.

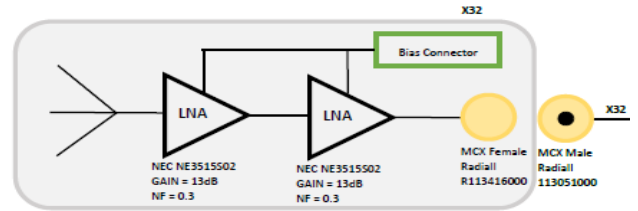


Figure 3: PAF front-end schematic.

Downstream of the system composed of the array and the LNAs, the design of a signal acquisition chain, which is composed of a conditioning circuit to adapt the signal levels to the ones accepted by the RFSOC, has been developed. This receiving chain is equipped with bandpass filters (with 4.6-6.2 GHz rejection band) in cascade with three additional amplification stages and a step attenuator, as shown in Figure 2 and 3.

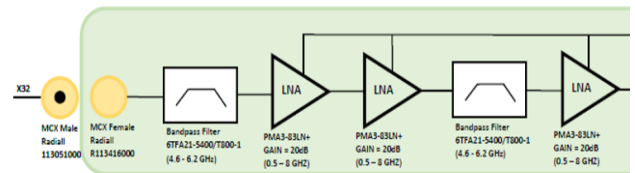


Figure 2: Signal acquisition chain of the front-end 1...

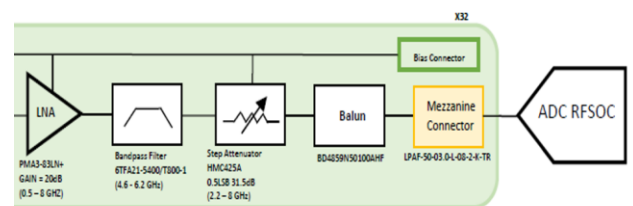


Figure 3: Signal acquisition chain of the front-end 2.

3 The design of the back-end based on the Xilinx ZCU216 RFSOC boards

The back-end of the system will be based on two Xilinx ZCU216 RFSOC boards connected each other with a 4 x 25G Ethernet cable and with an FMC+ 100 G with the server.

It is necessary to develop the firmware and software to configure the two boards with the aim to perform the data acquisition, filtering and beam-forming. Some blocks are ready as they have been developed in the CASPER framework.

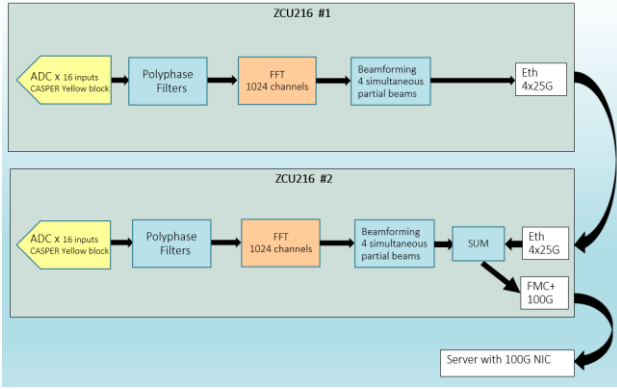


Figure 4: Digital beamformer schematic

4 Adaptive beam-forming using Deep-Learning Techniques

The advantages of the PAF are related to its pattern-synthesis capabilities, obtained by the electronic control of the phase and amplitude of the single antenna elements. By using specifically dedicated algorithms it is possible to create multiple beams optimizing the rate between the system temperature and the efficiency of the radio telescope, for example by putting nulls on the direction of Radio Frequency Interferences (RFIs).

Pattern-synthesis algorithms based on traditionally used optimization techniques are very flexible, but for their intrinsic iterative nature, may require a long time to converge to an optimal or sub-optimal solution, because a large number of iterations or complex computations for matrix inversions is typically required.

Our work, inspired by [12], investigates the possibility to use Convolution Neural Networks (CNNs) to perform this task, extracting the required features directly from the radiation patterns of the front-end (see Figure 5). The corresponding weights vectors, assigned to the antennas to obtain the patterns, are calculated using a classical optimization system taken as a reference and used as ground truth for the training process.

For the model to be well trained we build a dataset in part synthesized using a simulator and in part obtained from real observations [12]. By varying the direction of the main lobe and that of the RFI, to obtain very representative data, the network will be able to understand the problem, especially in mitigating the interferences.

Our study also proposes a comparison between different deep learning models to identify which architecture performs better in terms of computation time, directivity loss and interference suppression to mitigate, with the updated pattern, the effects of the interfering disturbances in quasi real-time (see Figure 5).

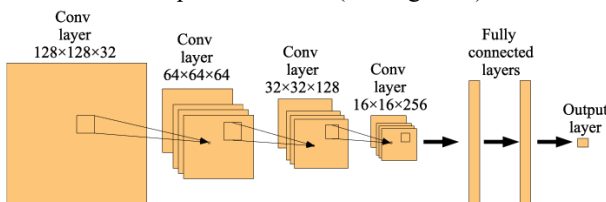


Figure 5: CNN classical architecture.

This paper's copyright is held by the author(s). It is published in these proceedings and included in any archive such as IEEE Xplore under the license granted by the "Agreement Granting URSI and IEICE Rights Related to Publication of Scholarly Work."

5 The optimizer for a Noise-Matched PAF

With the aim to evaluate the best performances of the whole PAF system, a model that compares the simulation predictions with measurements is analyzed. The approach derives from the studies of D. A. Roshi, who describes in [15] a model for a noise-matched PAF system and compares model predictions with the measurement results. The model was ad hoc developed for the 1.4 GHz, 19-element, dual-polarized PAF for the Robert C. Byrd Green Bank Telescope (GBT) [13] consisting of an array feed, a signal acquisition chain, a beam-former, and a parabolic reflector (in our case, we consider SRT). The whole PAF system can be characterized by a single matrix, constructed from the open-circuit voltage covariance (OCVC) at the output of the PAF due to a signal from the observing source, ground spillover noise, sky background noise, and LNAs noise. The best signal-to-noise ratio (SNR) on the source achievable with the PAF system will be the maximum eigenvalue of the characteristic matrix [13]. This model will be used for testing the system during observations.

6 Conclusions

The status of the new C-band PAF, which operates in the frequency range between 4.75 and 6 GHz, is presented. The design of the front-end involves the development of an array of $8 \times 8 \times 2$ (128) dual-polarization Vivaldi antennas, 32 of which are active and directly connected to the LNAs and to the signal acquisition chain. The RF signals of all active elements are injected into the back-end, based on two Xilinx ZCU216 RFSoc boards. The back-end permits the data acquisition, filtering and beam-forming, which could be performed using an approach based on deep learning techniques. Finally, an optimizer for evaluating the performances of the whole system is analyzed.

References

- [1] J.R.Fisher, R.F. Bradely, Full-sampling array feeds for radio telescopes. In Proceedings of the SPIE Astronomical Telescopes and Instrumentation, Munich, Germany, 3 July 2000.
- [2] K. Warnick, Maaskant, M.V. Ivashina, D.B. Davidson, R.B.D. Jeffs, High-Sensitivity Phased Array Receivers for Radio Astronomy. Proc. IEEE 2016, 104, 607–622.
- [3] A. Roshi, D. W. Shillue, B. Simon, K.F. Warnick, Jeffs, B. D.J. Pisano, R. Prestage, S. White, J.R. Fisher, M. Morgan, et al. Performance of a highly sensitive, 19-element, dual-polarization, cryogenic L-band phased array feed on the Green Bank Telescope. Astron. J. 2018, 155, 18.
- [4] A. Navarrini, A. Scalambra, S. Rusticelli, A. Maccaferri, A. Cattani, F. Perini, P. Ortu, J. Roda, P. Marongiu, A. Saba, M. Poloni, A. Ladu, L. Schirru, The Room Temperature Multi-Channel Heterodyne Receiver Section of the PHAROS2 Phased Array Feed. Electronics 2019, 8, 666. <https://doi.org/10.3390/electronics8060666>.

- [5] D.R. DeBoer, R.G. Gough, J.D. Bunton, T.J. Cornwell, R.J. Beresford, S. Johnston, I.J. Feain, A.E. Schinckel, C.A. Jackson, M.J. Kesteven, et al. Australian SKA Pathfinder: A High-Dynamic Range Wide-Field of View Survey Telescope. *Proc. IEEE* 2009, 97, 1507–1521.
- [6] B. Hut, R.H. van den Brink,; W.A. van Cappellen, Status update on the system validation of APERITIF, the phased array feed system for the Westerbork synthesis radio telescope. In *Proceedings of 11th European Conference on Antenna and Propagation (EUCAP)*, Paris, France, 19–24 March 2017.
- [7] A. Navarrini et al, “The Warm Receiver Section and the Digital Backend of the PHAROS2 Phased Array Feed,” *IEEE Int. Symp. on Phased Array Systems and Technologies (PAST)*, Waltham, MA, USA, Oct. 15-18, 2019.
- [8] L. Schirru, T. Pisanu, A. Navarrini, E. Urru, F. Gaudiomonte, P. Ortu, G. Montisci, Advantages of Using a C-band Phased Array Feed as a Receiver in the Sardinia Radio Telescope for Space Debris Monitoring. In *Proceedings of the 2019 IEEE 2nd Ukraine Conference on Electrical and Computer Engineering (UKRCON)*, Lviv, Ukraine, 2–6 July 2019.
- [9] A. Navarrini, R. Nesti, L. Schirru, Electromagnetic simulation and beam-pattern optimization of a C-band Phased Array Feed for the Sardinia Radio Telescope. In *Proceedings of the 2019 IEEE 2nd Ukraine Conference on Electrical and Computer Engineering (UKRCON)*, Lviv, Ukraine, 2–6 July 2019.
- [10] A. Navarrini et al., "Architecture of C-band Phased Array Feed with RFSoc digital beamformer," 2022 3rd URSI Atlantic and Asia Pacific Radio Science Meeting (AT-AP-RASC), Gran Canaria, Spain, 2022, pp. 1-3, doi: 10.23919/AT-AP-RASC54737.2022.9814401.
- [11] P. Bolli et al., “Sardinia Radio Telescope: General Description, Technical Commissioning and First Light”, *Journal of Astronomical Instrumentation*, **Vol. 4**, Nos. 3&4, doi: 10.1142/S2251171715500087.
- [12] S. Bianco et al. "AESAs Adaptive Beamforming Using Deep Learning," 2020 IEEE Radar Conference (RadarConf20), 2020.
- [13] D. A. Roshi, W. Shillue and J. R. Fisher, "Model for a Noise-Matched Phased Array Feed," in *IEEE Transactions on Antennas and Propagation*, vol. 67, no. 5, pp. 3011-3021, May 2019, doi: 10.1109/TAP.2019.2899046.